Comprehensive bioinformatics analysis to identify and validate potential prognostic markers for esophageal squamous carcinoma

Tao Tao, Qicai Li, Yifan Yang, Guowen Wang

Department of Thoracic Surgery, The First Affiliated Hospital of Bengbu Medical College, 233004, China

Introduction. Esophageal squamous cell carcinoma (ESCC) is a leading gastrointestinal malignancies with unclear molecular mechanisms. We try to screen genes associated with ESCC and find possible prognostic markers through integrative bioinformatic analysis to identify differentially expressed coding genes (DEGs).

Methods. Protein-protein interaction (PPI) networks for DEGs were created using Search Tool for Interacting Genes/Proteins (STRING) and visualised using Cytoscape. Survival analysis by long-rank analysis was adopted to estimate genes' potential prognostic value; real-time quantitative PCR (RT-qPCR) was used to detect gene expression in ESCC tissues. Clonogenic plate assay was performed to detect cell migration after ALOX12 knockdown, and Q-PCR was carried out to check cells' epithelial-mesenchymal transition (EMT) after ALOX12 knockdown.

Results. ???

Conclusion. ALOX12 knockdown drastically inhibited cells' migration via modulating EMT. ALOX12 may be a key gene and a potential prognostic biomarker for esophageal squamous carcinoma.

Keywords. Esophageal squamous carcinoma, RNA-seq, bioinformatics analysis, marker，EMT

INTRODUCTION

Having a survival rate of 15-25%, esophageal cancer is a leading lethal malignancy [1] that can be histologically grouped into esophageal squamous carcinoma (ESC) and esophageal adenocarcinoma (EAC) [2]. In China, 90% esophageal cancer cases are ESC [3]. An in-depth understanding of transcriptional dysregulation in esophageal

1

squamous carcinoma is essential to predict prognosis, provide appropriate treatment and improve clinical outcomes [4,5,6].

Second-generation sequencing technology is very helpful to ESCC transcriptional signature profiling and target gene screening [7,8]. Tong et al [9] included transcriptomic data from 7 ESC samples and 5 non-tumour samples to analyse ESC's transcriptional signature. Wang et al.[10] included RNA-seq data of 7 paired tumour/normal tissues to map the 'landscape' of incrna and messenger RNA in oesophageal squamous carcinoma. However, due to sample heterogeneity, RNA-seq results differ from experiment to experiment. In addition, small sample sizes limit these results' reproducibility and reliability.

Here, using RNA-seq technology, we studied the transcriptional characteristics of 3 paired ESC/normal mucosal tissues from Xiangya Hospital, Central South University. In addition, publically available RNA-seq datasets from GEO, including GSE32700, GSE39491 and GSE36223 were included to screen potential pathogenic genes. The GeneChip dataset for ESC (GSE53625) dataset for head and neck squamous cell carcinoma (TCGA_HNSCC) were adopted to assess prognostic values of 'pivotal' genes in the discovery dataset. ALOX12 was upregulated in esophageal squamous carcinoma and was identified as a potential prognostic marker, and in vitro experiments were conducted to elaborate its role and potential mechanisms.

MATERIALS AND METHODS

RNA-seq Data

GSE32700, GSE39491 and GSE36223 were from NCBI with reading Archive1 with identifier SRP133303 [10 10] and SRP008496 [11]. GSE32700 contained 14 normal specimens and 14 tumour specimens. GSE39491 contained 20 normal and 20 tumour tissues, and GSE36223 contained 30 normal and 30 tumour specimens.

Data Processing

Download RNA-seq data for tcga_escc from Firehose2. The RNA-seq datasets (GSE32700, GSE39491 and GSE36223) were defined as "discovery datasets". DEGs

2

between ESCC and normal controls were screened in all datasets using "DEseq2" R package (Vienna, Austria). DEGs were screened using the | log2(fold change) &gt criterion; false discovery rate (FDR) <0.01. Subsequently, volcano maps were drawn using the DEGs.

To explore DEGs' roles, "clusterProfiler" for enrichment analysis of the core gene and genome encyclopedia (KEGG) pathways and gene ontology (GO) analysis of 3 domains: cellular components (CC), biological processes (BP) and molecular functions (MF) [12].

Construction and Modular Analysis of Protein Interaction Networks

PPI networks were constructed by STRING to explore interrelationships between DECGs [13], with a medium confidence interval of 0.400. PPI networks were visualised using Cytoscape software. The highly interactive nodes in the subnetwork were identified using the MCODE [14] Cytoscape plugin with maximum depth= 100, degree= 2, node score= 0.2,k-core = 2.

Survival Analysis and Validation of Hub Genes

DEGs' prognostic values in the PPI network were explored by log-rank survival analysis in both GSE53625 and TCGA_HNSCC datasets via the Kaplan-Meier method. The optimal cut-off point for the time-series test was determined using X-Tile [15].

RT-qPCR was carried out as follows: 95℃, 10 min (hold phase), 40 x (95℃, 15 s, 60℃, 1 min), 95℃, 15 s and 75℃, 1 min (melting curve phase). β-actin was included as an internal reference. Analysis of the data by comparing the cycling threshold ($2^{-\Delta\Delta Ct}$) method.

Gene Enrichment

Roles of different biological pathways in patients with high/low levels of target genes were analyzed by GSEA with R 3.6.24 using TCGA_ESCC dataset. p & lt;0.05was defined as significant enrichment.

Cell Culture

ESC cell lines (KYSE30, KYSE150, KYSE410, Eca109 and TE-1) from Chinese

3

Academy of Sciences (Shanghai, China) were cultured in RPMI 1640 with 10% (Gibco) at 37◦ C.

Transfection of siRNAs

Two small interfering rna and one scramble siRNA against ALOX12 were from Suzhou Gene Pharma. Silencing efficiency was detected by RT-qPCR 2-3 days later.

Determination of Cell Migration Capacity in Vitro

Transwell experiments were performed in 8μm Transwell chambers. Briefly, 1 day after siRNA transfection, 5×10^4 cells in 200 μL serum-free medium was inoculated in upper part, 800 μL of RPMI 1640 with 20% FBS was placed in lower part. After 2 days culture, cells on upper surface were swabbed prior to fixation and staining.

Immunoblotting

Equal amounts of protein lysate were resolved by SDS-PAGE and then immuno-probed with 1st antibody and HRP-labelled 2nd antibody.

Statistical Analysis

Data was analyzed by R 3.6.2 or Prism7 (GraphPad). t-test was used to compare continuous variables. Log-rank test was adopted for survival analysis. p & lt; at 0.05 was defined as statistically significant.

RESULTS

Identification of DEGs

Fig. 1 shows the flow chart of data processing and analysis in our study. The data sources were GSE32700, GSE39491 and GSE36223) for the analysis.

There were 103 DEGs in the GSE3270 dataset (29 up and 74 down), 1261 DEGs in the GSE39491 dataset (371 up and 890 down), and 846 DEGs in the GSE36223 dataset (256 up and 590 down) (Fig. 2A-D). Venn diagram indicated that 148 genes (106 up-regulated and 42 down-regulated) were differentially expressed in 4 datasets (Fig. 2E-F).
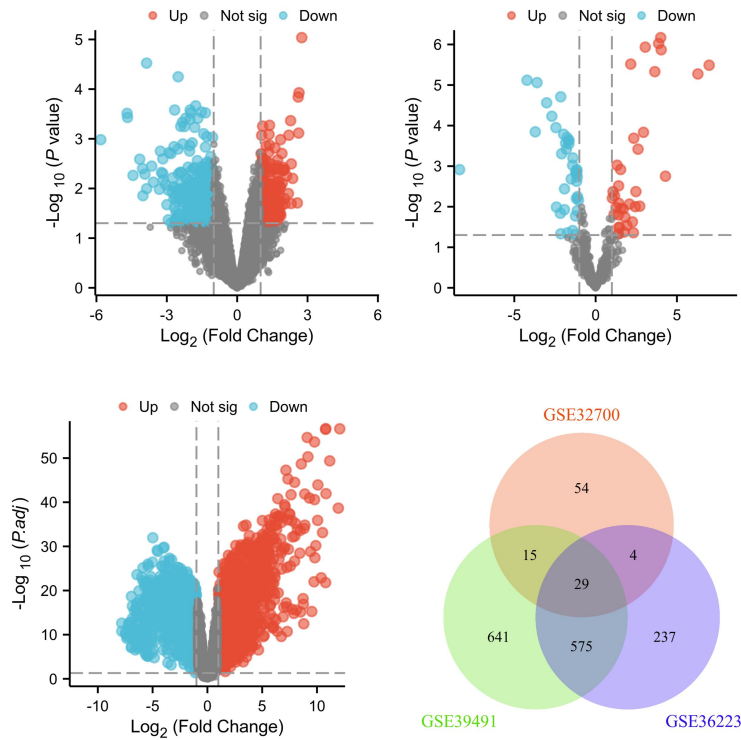
Fig. 2 DEGs in ESC|(A - D) Volcano plot of DEGs from GSE32700(A), GSE39491(B) and GSE36223(C). Black circles: non-differentially expressed genes (FDR >0.01), red circles: differentially expressed mrna [log2(fold change) >1 and FDR < blue circles: down-regulated differentially expressed mrna [log2(fold change) <1 and FDR <1;0.01]. Top 20 up- and down-regulated genes. (E,F) Venn diagram,, from three data sets.

Functional Analysis of DEGs

GO annotation analysis revealed that upregulated DECGs were enriched in extracellular structural organization (GO: BP), collagen-containing extracellular matrix (ECM)(GO: CC) and ECM structural composition (GO: MF (Fig. 3A). In the KEGG pathway analysis, upregulated genes were significantly enriched in proteoglycans and microrna (Fig. 3B). In addition, while down-regulated genes were in fatty acid metabolism (GO:BP), actin cytoskeleton (GO:CC) and arachidonic acid

5

monooxygenase activity (GO:MF) (Fig. 3C). kegg pathway analysis showed that down-regulated genes were significantly enriched in arachidonic acid metabolism and chemical aspects of carcinogenesis (Fig. 3).
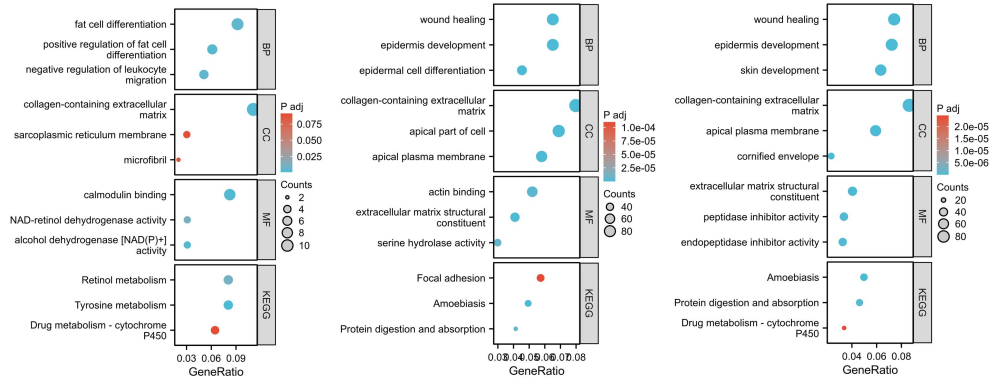

Fig. 3 | GO and KEGG analysis of DEGs (A - C) GO annotation of upregulated DEGs in terms of BP (A), CC (B) and MF (C). (D) KEGG pathway analysis of the up-regulated DEGs. (E - G) GO annotation analysis of down-regulated DEGs in 3 domains: BP (E), CC (F) and MF (G). (H) KEGG pathway analysis of down-regulated DEGs. Point sizes represent the number of genes; colours indicate adjusted p-values.

PPI Network Construction, Module Analysis and Hub Gene Selection

A PPI network with 3 nodes and 4 edges was established by inputting 29 genes to STRING and visualised by Cytoscape (Fig. 4A). Rectangles indicate up-regulated genes and diamonds represent down-regulated genes in ESC tissue. MCODE Cytoscape plugin pointed out 2 modules (Fig. 4B-C). KEGG suggested that #1 enriched for ECM-receptor interactions and adhesive patches (Fig. 4D), while #2 enriched for DNA replication (Fig. 4E).
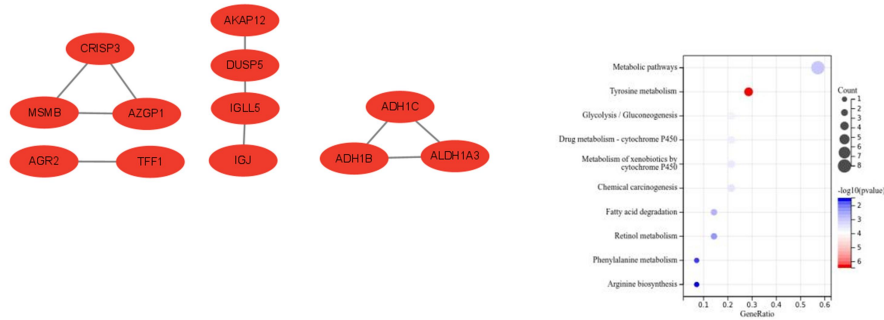
6

Fig. 4. PPI network of DEGs. Rectangles and diamonds represent genes up- or down-regulated in ESCC. (B,C) Two modules from MCODE Cytoscape; KEGG analysis showing module 1 or 2 was enriched in ecm-receptor interactions (D) or DNA replication (E).

Hub Gene Confirmation in ESCC

Further study of the prognostic value of key genes expression RT-qPCR to detect esophageal squamous carcinoma Screening of CRISP3, AGR2, ALOX12, IGJ, LDB2, ADH1C, RNASE1 expression in esophageal squamous carcinoma tissues Non-cancerous esophageal tissue specimens. the expression of CRISP3, AGR2, ALOX12, IGJ, LDB2, ADH1C, and RNASE1 were higher in ESC than that of non-tumor tissues (Fig. 6).
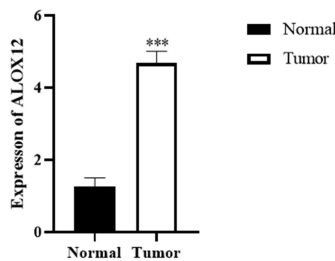

Fig. 6 | RT-qPCR revealed that ALOX12 was significantly higher in ESCC than non-tumor tissues (P <0.05). nc, negative control.

ALOX12 Silencing Cell Metastasis by Regulating EMT

Data indicated that EMT genes were directly related to ALOX12 (NES 3.894, P =

0.006; ALOX12 levels were measured by RT-PCR in KYSE150) (Fig. 7A). We selected this one cell line for subsequent experiments. Transfection of si-ALOX12 #1 or #2 significant suppressed ALOX12 (Fig. 7B-C). Silencing ALOX12 also inhibited cell migration (P <0.001, Fig. 7D-E). Immunoblotting revealed that silencing ALOX12 decreased N-cadherin expression (Fig. 7FG). We also explored the role of ALOX12 in esophageal squamous carcinoma, Silencing ALOX12 also drastically reduced cell migration without affecting EMT.
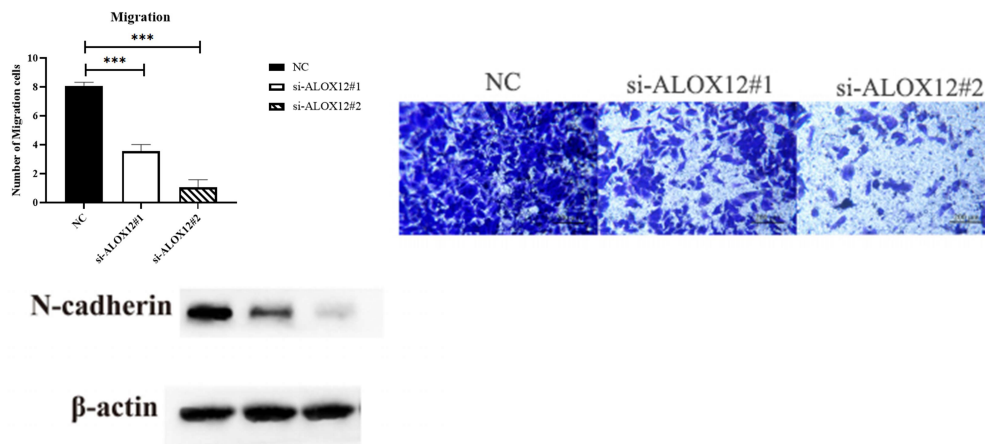

Fig. 7 | (A) In 1 candidate ESCC cell line (KYSE410), the expression was relatively high, so both cell lines were selected for subsequent experiments. (B)Down-regulation of ALOX12 suppressed ESCC cell migration. (C) Knockdown of ALOX12 expression reduced N-cadherin expression in Eca109 and KYSE410 cells. * * * P & lt;0.001

DISCUSSION

Studying the molecular mechanisms of ESC has important implications for prognostic prediction. We found 6 and 23 genes were up- or down-regulated and their roles were further assessed. One significant module was screened from a 54 protein-containing PPI network using Cytoscape MCODE plugin.

Prognostic values of key genes were explored using GSE53625 dataset. high expression of ALOX12 among the 10 core proteins of module 1 suggests poor

prognosis. ALOX12 is an important ECM component and is closely related to cell migration and tumor progression [21,23]. Numerous results suggested that ALOX12 regulated the progression and metastasis of several malignancies, such as prostate [24], stomach [25], endometrium [26] and colon cancer [29,30,31]. Similarly, bone bridging protein is associated with tumour metastasis and poor prognosis [31,32,33]. However, the prognostic value of the 6 up-regulated RNAs did not show good prognostic values due to the lack of RNA probes GSE53625 microarray platform.

In addition, a previous study showed that matched healthy individuals with normal values differed from paired normal tissues taken from patients [34,35]. In the present study, we initially screened paired normal/tumor tissues in TCGA datasets for DEGs. We then also analysed the database of DEGs between TCGA and GTEx (gene profiling of healthy people) (Fig. 4A). Data showed a significantly higher number of DEGs compared to normal tissues (Fig. 4B). The number of overlapping genes were 521. In addition, we showed that a total of 125 genes had the same expression pattern. Of note was the ALOX12 gene for analysis.

It has been reported that ESCC and HNSCC can be considered as a single disease based on multi-platforms, such as somatic cell copy number alterations, DNA methylation and transcription. They both are squamous cell carcinoma that occurred in upper esophagus and smoking and alcohol are their risk factors [36,37]. In addition, expression of key genes similar to those found in ESC was revealed in TCGA_HNSCC. Therefore, joint analysis of data from ESC and HNSCC is a promising approach to explore ESC's characteristics. Furthermore, same results were seen from either TCGA_HNSCC or GSE53625 dataset (such as high levels of SPP1 and BGN in both datasets indicated poorer overall survival). In addition, overexpression of ALOX12 was related to poor prognosis in both HNSCC and ESCC. To confirm the finding, we examined the expression of the key gene ALOX12 in clinical tumour samples using RT-qPCR. Those genes had drastically higher levels in tumor than in normal tissue, confirming bioinformatic findings.

ALOX12 interacts with and inhibits NF-κB pathway in a variety of cancers, such as

mammary cancer[38,39,40], melanoma[41], non-small cell lung cancer (NSCLC)[42], nasopharyngeal carcinoma[43], laryngeal cancer[44] and esophageal squamous carcinoma[45].

It has been indicated that ALOX12's high levels contributed to poor prognosis in mammary cancer [46] and NSCLC [47,48]. microRNA-217 regulates ALOX12 expression and upregulates Forkhead Box Protein P1 (FOXP1) expression to promote lung adenocarcinogenesis [49,50]. However, how ALOX12 functions in ESCC is unclear. This study suggested that silencing ALOX12 (i) sharply inhibited ESCC cell migration and (ii) reduced its EMT markers. Taken together, ALOX12 is a novel oncogene in ESCC and critically regulates ESCC cell metastasis.

CONCLUSION

In summary, by integrating transcriptomic data analysis, 1 core protein-encoding gene (ALOX12) was found as a potential pathogenic gene and prognostic marker in esophageal squamous carcinoma. Furthermore, GSEA showed that ALOX12 was positively associated with EMT. Silencing ALOX12 inhibited the ability of ESC cells to migrate by regulating EMT.

It is worth to note the limitation of small sample size and patient loss of access. In addition, the regulatory mechanism of ALOX12 in esophageal squamous carcinoma is unclear. Therefore, large-size clinical data and mechanism studies are needed to elucidate how ALOX12 functions in ESCC.

DECLARATIONS

Competing of Interest

The authors declared that they have no conflicts of interest regarding the publication of this paper.

Data Availability Statement

The data that support the findings of this study are available from the corresponding author upon reasonable request. This study analysed publicly available datasets. The data can be found here: https://www.ncbi.nlm.nih.gov.

Funding Details

REFERENCES

[1] Bandettini, W. P., Kellman, P., Mancini, C., Booker, O. J., Vasu, S., Leung, S. W.,et al. (2012). MultiContrast delayed enhancement (Mcode) improves detection of subendocardial myocardial infarction by late gadolinium enhancement cardiovascular magnetic resonance: a clinical validation study. J. Cardiovasc. Magn. Reson. 14:83.

[2] Bian, D., Gao, C., Bao, K., and Song, G. (2017). The long non-coding RNA NKILA inhibits the invasion-metastasis cascade of malignant melanoma via the regulation of NF-kB. Am. J. Cancer Res. 7, 28–40.

[3] Briones-Orta, M. A., Avendano-Vazquez, S. E., Aparicio-Bautista, D. I., Coombes, J. D., Weber, G. F., and Syn, W. K. (2017). Osteopontin splice variants and polymorphisms in cancer progression and prognosis. Biochim. Biophys. Acta Rev. Cancer 1868, 93–108.A. doi: 10.1016/j.bbcan.2017.02.005.

[4] Buzdin, A., Sorokin, M., Garazha, A., Sekacheva, M., Kim, E., Zhukov, N., et al. (2018). Molecular pathway activation - New type of biomarkers for tumor morphology and personalized selection of target drugs. Semin. Cancer Biol. 53, 110–124. doi: 10.1016/j.semcancer.2018.06.003.

[5] Cabiati, M., Gaggini, M., Cesare, M. M., Caselli, C., De Simone, P., Filipponi, F., et al. (2017). Osteopontin in hepatocellular carcinoma: a possible biomarker for diagnosis and follow-up. Cytokine 99, 59–65. doi: 10.1016/j.cyto.2017.07.004.

[6] Wang, W., Wei, C., Li, P., Wang, L., Li, W., Chen, K., et al. (2018). Integrative analysis of mRNA and lncRNA profiles identified pathogenetic RNAs in esophageal squamous cell carcinoma. Gene 661, 169–175. doi: 10.1016/j.gene.2018.03.066.

[7] Huang, J., Wang, G., Tang, J., Zhuang, W., Wang, L. P., Liou, Y. L., et al. (2017). DNA methylation status of PAX1 and ZNF582 in esophageal squamous cell carcinoma. Int. J. Environ. Res. Public Health 14:216. doi: 10.3390/ijerph14020216.

[8] Kim, D., Langmead, B., and Salzberg, S. L. (2015). HISAT: a fast spliced aligner with low memory requirements. Nat. Methods 12, 357–360.

[9] Wu, W., Chen, F., Cui, X., Yang, L., Chen, J., Zhao, J., et al. (2018). RNA NKILA suppresses

TGF-beta-induced epithelial-mesenchymal transition by blocking NF-kappaB signaling in breast cancer. Int. J. Cancer 143, 2213–2224. doi: 10.1002/ijc.31605.

[10] Dixon SJ et al. Ferroptosis: an iron-dependent form of nonapoptotic cell death. Cell 149, 1060–1072, doi: 10.1016/j.cell.2012.03.042 (2012).

[11] Zhang YL et al. BAP1 links metabolic regulation of ferroptosis to tumour suppression. Nat Cell Biol 20, 1181–1192, doi: 10.1038/s41556-018-0178-0 (2018).

[12] Angeli JPF, Shah R, Pratt DA & Conrad M Ferroptosis Inhibition: Mechanisms and Opportunities. Trends Pharmacol Sci 38, 489–498, doi: 10.1016/j.tips.2017.02.005

[13] Viswanathan VS et al. (2017)Dependency of a therapy-resistant state of cancer cells on a lipid peroxidase pathway. Nature 547, 453–457, doi: 10.1038/nature23007.

[14] Ingold I et al. Expression of a Catalytically Inactive Mutant Form of Glutathione Peroxidase 4 (Gpx4) Confers a Dominant-negative Effect in Male Fertility. J Biol Chem 290, 14668–14678, doi: 10.1074/jbc.M115.656363 .

[15] Schriever SC et al. Alterations in Neuronal Control of Body Weight and Anxiety Behavior by Glutathione Peroxidase 4 Deficiency. Neuroscience 357, 241–254, doi: 10.1016/j.neuroscience.2017.05.050.

[16] Yang WS et al. Regulation of Ferroptotic Cancer Cell Death by GPX4. Cell 156, 317–331, doi: 10.1016/j.cell.2013.12.010.

[17] Imai H, Matsuoka M, Kumagai T, Sakamoto T & Koumura T Lipid Peroxidation-Dependent Cell Death Regulated by GPx4 and Ferroptosis. Curr Top Microbiol 403, 143–170.

[18] Dixon SJ et al., Human Haploid Cell Genetics Reveals Roles for Lipid Metabolism Genes in Nonapoptotic Cell Death. ACS Chem Biol. 10, 1604–9. doi: 10.1021/acschembio.5b00245.

[19] Eischen CM, Weber JD, Roussel MF, Sherr CJ & Cleveland JL Disruption of the ARF-Mdm2-p53 tumor suppressor pathway in Myc-induced lymphomagenesis. Genes & development 13, 2658–2669, doi:DOI 10.1101/gad.13.20.2658

[20] Liu Y et al. Deletions linked to TP53 loss drive cancer through p53-independent mechanisms. Nature 531, 471–457, doi: 10.1038/nature17157.

[21] Gasol E, Jimenez-Vidal M, Chillaron J, Zorzano A & Palacin M Membrane topology of system xc- light subunit reveals a re-entrant loop with substrate-restricted accessibility. J Biol Chem 279,

31228–31236, doi: 10.1074/jbc.M402428200.

[22] Dixon SJ et al. Pharmacological inhibition of cystine-glutamate exchange induces endoplasmic reticulum stress and ferroptosis. Elife 3, doi:ARTN e02523 10.7554/eLife.02523.

[23] Kagan VE et al. Oxidized arachidonic and adrenic PEs navigate cells to ferroptosis. Nat Chem Biol 13, 81–90, doi: 10.1038/Nchembio.2238.

[24] Tarangelo A et al. p53 Suppresses Metabolic Stress-Induced Ferroptosis in Cancer Cells. Cell Rep 22, 569–575, doi: 10.1016/j.celrep.2017.12.077.

[25] Ferretti E, De Smaele E, Di Marcotullio L, Screpanti I & Gulino A Hedgehog checkpoints in medulloblastoma: the chromosome 17p deletion paradigm. Trends Mol Med 11, 537–545, doi: 10.1016/j.molmed.2005.10.005.

[26] Tam CS & Stilgenbauer S How best to manage patients with chronic lymphocytic leuekmia with 17p deletion and/or TP53 mutation? Leukemia Lymphoma 56, 587–593, doi: 10.3109/10428194.2015.1011641.

[27] Ingold I, et al., (2018) Selenium Utilization by GPX4 Is Required to Prevent Hydroperoxide-Induced Ferroptosis. Cell. 172, 409–422.

[28] Johnson EN, Brass LF & Funk CD Increased platelet sensitivity to ADP in mice lacking platelet-type 12-lipoxygenase. Proceedings of the National Academy of Sciences of the United States of America 95, 3100–3105.

[29] Bensaad K et al. TIGAR, a p53-inducible regulator of glycolysis and apoptosis. Cell 126, 107–120, doi: 10.1016/j.cell.2006.05.036.

[30] Kruiswijk F, Labuschagne CF, Vousden KH p53 in survival, death and metabolic health: a lifeguard with a licence to kill. Nat Rev Mol Cell Biol. 7, 393–405.

[31] Hughes RH, Silva VA, Ahmed I, Shreiber DI & Morrison B 3rd Neuroprotection by genipin against reactive oxygen and reactive nitrogen species-mediated injury in organotypic hippocampal slice cultures. Brain research 1543, 308–314.

[32] Wang Z, Jiang H, Chen S, Du F & Wang X The mitochondrial phosphatase PGAM5 functions at the convergence point of multiple necrotic death pathways. Cell 148, 228–243.

[33] Xu, C., Sun, L., Jiang, C., Zhou, H., Gu, L., Liu, Y., et al. (2017). SPP1, analyzed by bioinformatics methods, promotes the metastasis in colorectal cancer by activating EMT pathway.

Biomed. Pharmacother. 91, 1167–1177. doi: 10.1016/j.biopha.2017.05.056.

[34] Yang, T., Li, S., Liu, J., Yin, D., Yang, X., and Tang, Q. (2018). RNA-NKILA/NFkappaB feedback loop modulates laryngeal cancer cell proliferation, invasion, and radioresistance. Cancer Med. 7, 2048–2063. doi: 10.1002/cam4.1405.

[35] Liu, A. N., Qu, H. J., Yu, C. Y., and Sun, P. (2018). Knockdown of ALOX12 inhibits lung adenocarcinoma cell progression by up-regulating miR-217 and down-regulating FOXP1. J. Cell Mol. Med. 22, 4034–4044. doi: 10.1111/jcmm.13483.

[36] Lu, Z., Chen, Z., Li, Y., Wang, J., Zhang, Z., Che, Y., et al. (2018). TGF-beta-induced NKILA inhibits ESCC cell migration and invasion through NF-kappaB/MMP14 signaling. J. Mol. Med. 96, 301–313. doi: 10.1007/s00109-018-1621-1.

[37] Peng, H. H., Zhang, X., and Cao, P. G. (2012). MMP-1/PAR-1 signal transduction axis and its prognostic impact in esophageal squamous cell carcinoma. Braz. J. Med. Biol. Res. 45, 86–92. doi: 10.1590/s0100-879x2011007500152.

[38] Sun, H., Wang, X., Zhang, Y., Che, X., Liu, Z., Zhang, L., et al. (2016). Biglycan enhances the ability of migration and invasion in endometrial cancer. Arch. Gynecol. Obstet. 293, 429–438. doi: 10.1007/s00404-015-3844-5.

[39] Zhao, L., Chi, W., Cao, H., Cui, W., Meng, W., Guo, W., et al. (2019). Screening and clinical significance of tumor markers in head and neck squamous cell carcinoma through bioinformatics analysis. Mol. Med. Rep. 19, 143–154. doi:10.3892/mmr.2018.9639.

[40] Tarangelo A et al. p53 Suppresses Metabolic Stress-Induced Ferroptosis in Cancer Cells. Cell Rep 22, 569–575, doi: 10.1016/j.celrep.2017.12.077.

[41] Post SM et al. p53-dependent senescence delays E mu-myc-induced B-cell lymphomagenesis. Oncogene 29, 1260–1269, doi: 10.1038/onc.2009.423.

[42] Eischen CM, Weber JD, Roussel MF, Sherr CJ & Cleveland JL Disruption of the ARF-Mdm2-p53 tumor suppressor pathway in Myc-induced lymphomagenesis. Genes & development 13, 2658–2669, doi:DOI 10.1101/gad.13.20.2658.

[43] Imai H, Matsuoka M, Kumagai T, Sakamoto T & Koumura T Lipid Peroxidation-Dependent Cell Death Regulated by GPx4 and Ferroptosis. Curr Top Microbiol 403, 143–170, doi: 10.1007/82_2016_508.

[44] Schriever SC et al. Alterations in Neuronal Control of Body Weight and Anxiety Behavior by Glutathione Peroxidase 4 Deficiency. Neuroscience 357, 241–254, doi: 10.1016/j.neuroscience.2017.05.050.

[45] Angeli JPF et al. Inactivation of the ferroptosis regulator Gpx4 triggers acute renal failure in mice. Nat Cell Biol 16, 1180–U1120, doi: 10.1038/ncb3064.

[46] Dixon SJ et al. Ferroptosis: an iron-dependent form of nonapoptotic cell death. Cell 149, 1060–1072, doi: 10.1016/j.cell.2012.03.042.

[47] Zhang, H., Chen, W., Duan, C. J., and Zhang, C. F. (2013).). Overexpression of HSPA2 is correlated with poor prognosis in esophageal squamous cell carcinoma. World J. Surg. Oncol. 11:141. doi: 10.1186/1477-7819-11-141.

[48] Xu, C., Sun, L., Jiang, C., Zhou, H., Gu, L., Liu, Y., et al. (2017). SPP1, analyzed by bioinformatics methods, promotes the metastasis in colorectal cancer by activating EMT pathway. Biomed. Pharmacother. 91, 1167–1177. doi: 10.1016/j.biopha.2017.05.056.

[49] Jacobsen, F., Kraft, J., Schroeder, C., Hube-Magg, C., Kluth, M., Lang, D. S.,et al. (2017). Up-regulation of Biglycan is Associated with Poor Prognosis and PTEN Deletion in Patients with Prostate Cancer. Neoplasia 19, 707–715.doi: 10.1016/j.neo.2017.06.003.

[50] Hu, L., Zang, M. D., Wang, H. X., Li, J. F., Su, L. P., Yan, M., et al. (2016). Biglycan stimulates VEGF expression in endothelial cells by activating the TLR signaling pathway. Mol. Oncol. 10, 1473–1484. doi: 10.1016/j.molonc.2016.08.002.

Corresponding Author:
Guowen Wang
No.287, Changhuai Road, Bengbu City, Anhui Province, China
E-mail:wgwzj@163.com

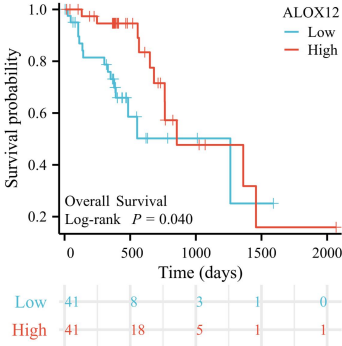Potential prognostic markers for esophageal squamous carcinoma—Tao et al

Fig. 5. | Log-rank test survival analysis; high levels of ALOX12 correlate with poor survival.